CHALMERS

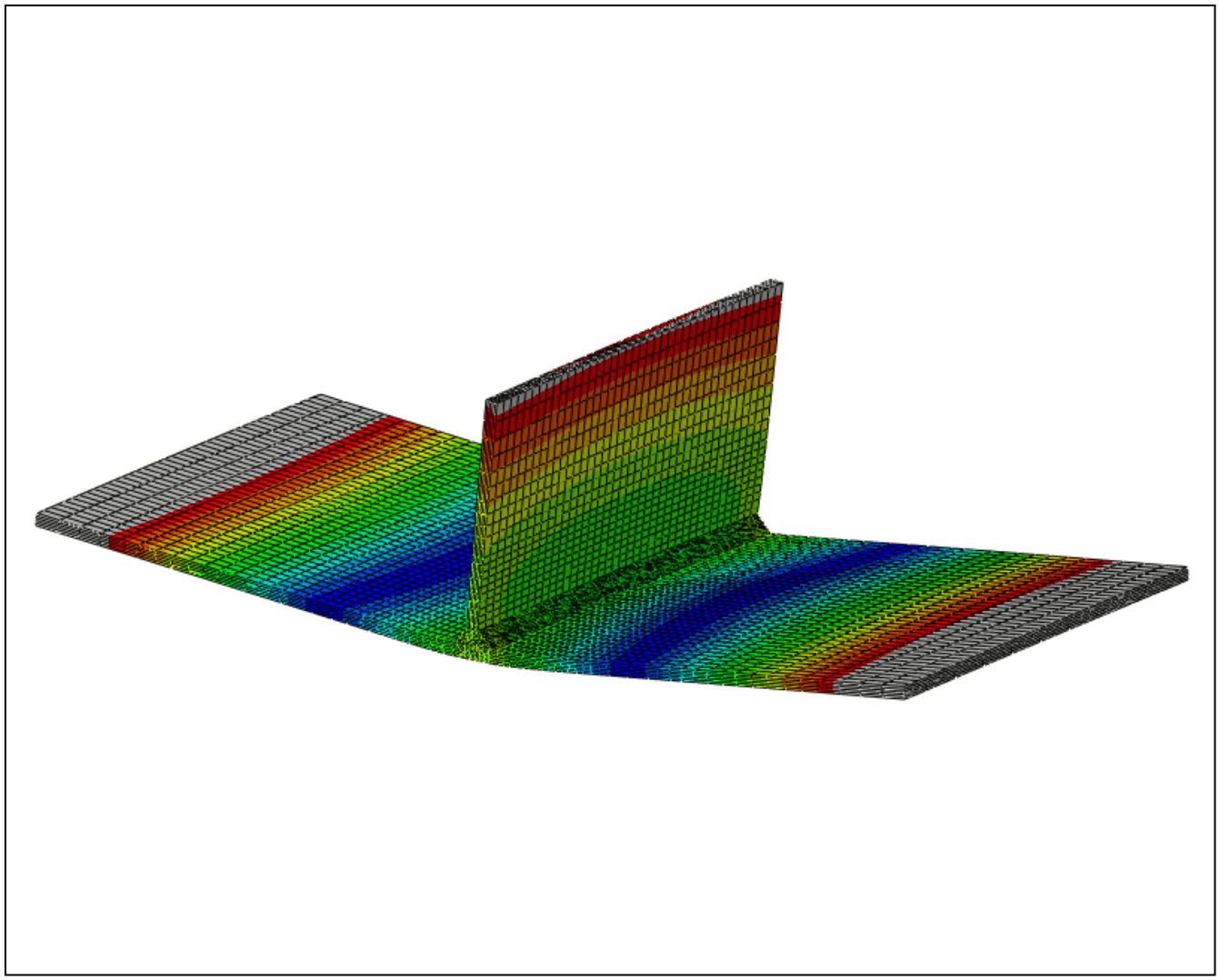

Studentarbeten – Mekanik och maritima vetenskaper (M2) – Projektarbeten 2020:02

Deformations in welded panels

TME131 Project in Applied Mechanics 2020

Department of Mechanics and Maritime Sciences
CHALMERS UNIVERSITY OF TECHNOLOGY
Göteborg, Sweden 2020

Deformations in welded panels
TME131 Project in Applied Mechanics 2020

Studentarbeten – Mekanik och maritima vetenskaper (M2) – Projektarbeten 2020:02

Department of Mechanics and Maritime Sciences
Chalmers University of Technology
SE-412 96 Göteborg
Sweden
Telephone +46 (0)31 772 1000

Preface

The work in the present report was carried out as a part of the course TME131 Project in Applied Mechanics, which is a mandatory course within the Applied Mechanics Masters programme at Chalmers. The course was carried out during spring semester 2020.

The project was supervised by Prof. Lennart Josefson (Chalmers University of Technology) and Prof. Em Moyra McDill (Carleton University).

Abstract

Welded panels are commonly used for ships hull manufacturing, and in order to lighten the hull the stiffened panel thickness tends to be reduced, thus increasing the distortion effects due to welding. This project will be part of Chalmers contribution to the benchmark exercise in a specialist committee, Material and Fabrication Technology, for the International Ship and Offshore Structures Congress (ISSC) 2021 conference. The project's purpose is to compute the deformation for the ISSC2021v.3 benchmark [1] geometry of a stiffened welded panel which comprises of a stiffener 1000 x 100 x 5 mm DH36 plate which is initially tack welded on one side to a 1000 x 400 x 5 mm DH36. The welding procedure consists of a first weld fillet being deposited on one side of the stiffener, followed by a cooling time, and then another weld fillet being deposited on the other side and followed by a second cooling time before the welded panel is finally unclamped. To achieve that, both thermal and mechanical analyses are carried out by relying on the nonlinear Finite Element Analysis (FEA). The commercial FEA program ABAQUS is used for analyses in this project. Those simulations are however performed for a shorter plate and stiffener of length 200 mm.

The material properties were implemented in ABAQUS input file form, for both the weld and the plate and stiffener. Nonlinear thermal and mechanical properties were taken into account. The specific heat and thermal conductivity were implemented for the DH36 steel, however other properties such as thermal expansion coefficient, Poisson's ratio etc., were implemented for a similar steel, S355. The weld material and the plate and stiffener are altogether modelled as being the same material except regarding the hardening modulus and the yield stress. When compared to the plate and stiffener material, the weld material itself has been modelled as having a higher yield stress and higher hardening modulus at room temperature.

Two thermal models are considered with each having 1000 °C as the heat source temperature of the weld. First, the fillet weld is activated simultaneously and in the second, the fillet weld material is activated sequentially by dividing the weld into segments. After each weld pass the model is allowed to cool down for 200 seconds so that the welded panel has cooled to around 50 °C at the end of the simulation.

The thermal simulations are coupled to mechanical simulations. In mechanical simulations, different clamping sequences are carried out. One with fully fixed and two with sliding clamps. In total six configurations are considered, since there are two thermal models and three clamping conditions for the mechanical simulations. Clamping is taken care of by taking the top and bottom nodes of the plate at designated locations.

The same mesh model was used for both the thermal and mechanical simulations, and it consists of linear 8-node hexahedral and linear 4-node tetrahedral solid elements. The linear hexahedral elements are used to model the plate and stiffener and the welding joint is modelled by linear tetrahedral elements. Prior to choosing

a final mesh a mesh convergence study was conducted by monitoring the temperature variation at a location close to the weld. The resulting mesh had 31200 nodes and elements with an aspect ratio lower than 10 to avoid complications with the mechanical simulations.

The results of this project showed that the type of heating source and the clamping conditions have definite effects on the behaviour of the model. The displacements results for the mechanical simulations indicated that the sequential heating results were closer to the intended ones than for the simultaneous heating case. Also, the extent of clamping conditions, i.e., either fully clamped or sliding clamps, along with the methods used to prevent rigid body motions for a sliding clamp are all factors which have an effect on the behaviour of the model. And these differences in the thermal and mechanical loading configurations will be magnified when they are applied to the full length of 1000 mm for the plate and stiffener as per the ISSC2021v.3 benchmark.

Keywords: ABAQUS, FEA, DH36, Inertia relief, Simultaneous, Sequential

Acknowledgements

We would like to thank our supervisors Lennart Josefsson and Moyra McDill for their valuable and constructive guidance during the planning and development of the project. We would also like to thank Björn Andersson for all the help and time he spent answering questions and tracking down issues with the simulations.

Daniel Hård, Bogdan Pamfil, Shivaprasad Gurram, Srikannan Selvaraj, May 2020

Contents

List of Figures

List of Tables

1 Introduction

A ship hull contains stiffened panels, see Figures 1.1a and 1.1b. The panels are constructed by welding them together using Gas Metal Arc Welding (GMAW) [2]. This means that molten material is deposited at the edges of the plates to join them together. The edges are locally heated up followed by rapid cooling resulting in local yielding. Plastic strains will be developed locally leading to residual stresses and deformations in the panel as shown in Figure 1.1.

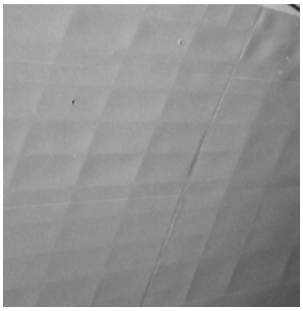

(a) Deformed panels of a ship hull.

(b) Stiffened panel on the inside of ship hull.

Figure 1.1: Structure of a ship hull with stiffened panels and deformations [2].

When designing ships it is important to control the weight of the ship as it affects the buoyancy and its load carrying capacity and thus affecting its intended purposes. Also reducing the material consumption is of interest because of economic and environmental reasons. One way of achieving this is by reducing the thickness of stiffened panels in the ship hull which are used in place of very thick sheets of metal. But reducing the thickness of even the stiffened panels might lead to increased residual deformations in the panels after the welding process, see Figure 1.1b. Some of the consequences of this are: poor fabrication issues, increased risk of buckling and encountering aesthetic problems.

As part of the course TME131 in Applied mechanics this project will contribute to a benchmark exercise in a Specialist Committee, V.3 Materials and Fabrication Technology for the International Ship and Offshore Structures Congress (ISSC) 2021 Conference [1]. The benchmark is to be carried out on a specified geometry of a stiffened panel, see Figure 3.1, by using nonlinear Finite Element Analysis (FEA) thermo-mechanical calculations in ABAQUS [3]. The first step is to create a thermal model simulating the welding process and then calculating a temperature distribution. This distribution will then be used as input to calculate the mechanical

deformations in the specified stiffened panel.

2 Project definition

The objective of the project is to determine the deformation in welded panels, by using nonlinear Finite Element Analysis (FEA). To lighten the ship hull, the stiffened panel thickness tends to be reduced, thus increasing the distortion effects due to welding. In order to find the deformation both thermal and mechanical analyses are carried out. The commercial FEA program ABAQUS [3] is used for the analysis in this project.

The task is in the form of a progressive analysis, divided into two stages. Firstly, a thermal analysis of welding is carried out by the use of either a modelled moving heat source or a simultaneous heat addition along the weld length. The second stage involves the mechanical simulation by modelling the mechanical boundary conditions to evaluate the residual deformations in the welded panel.

2.1 Goals

The goal of the project is to assess several simplified approaches based on thermal and mechanical simulations of a fillet welded stiffened panel manufactured with DH36 steel. The results are to be compared with the benchmark and they could suggest future strategies for developing similar test procedures.

This will be part of Chalmers' contribution to the benchmark exercise in a specialist commitee, Material and Fabrication Technology, for the International Ship and Offshore Structures Congress (ISSC) 2021 conference.

2.2 Goals Completed

The specific project goals have been achieved during this project:
• The CAD model has been created in ABAQUS to simulate both thermal and mechanical analysis
• A Mesh convergence study has been carried out with different mesh sizes and optimal mesh size is chosen from the convergence study.
• Thermal analysis have been carried out by applying proper boundary conditions and simulations has been performed for both simultaneous and sequential heat source models.
• Mechanical analysis have been carried out by constraining the nodes depending upon the boundary conditions (BCs). Simulations have also been performed by varying the clamping conditions and the deformations are analysed for those clamping conditions.
• The deformations obtained from the simulations have been compared to those from the experimental benchmark exercise and analytical solutions that are available in

the literature.

3 Methods

3.1 Geometry

The ISSC2021v.3 benchmark [1] geometry comprises of a stiffener 1000 x 100 x 5 mm DH36 plate which is initially tack welded on one side to a 1000 x 400 x 5 mm DH36 (DH36 is a structural steel mainly used for ship building) plate with run on/off tabs as shown in Figure 3.1. In this project a shorter plate and stiffener of length 200 mm was used due to constraints in time and resources. During the course of the project the ISSC2021v.3 benchmark exercise modified the welding sequence described in the planning report. Hence, the plate was first clamped in all positions, then the first weld was activated. The plate and stiffener cooled down to around 50 °C, then the second weld was activated in the opposite direction. When the second pass had cooled to some 50 °C the clamps were released.

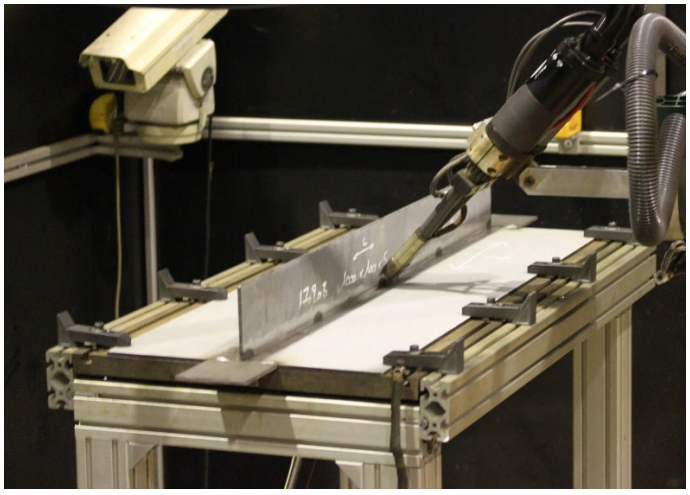

Figure 3.1: The welding experiment defined in the ISSC2021V.3 benchmark [1].

Clamping was assumed to mean either that the displacements are zero in all three directions at the point of clamping, or alternatively that only the out-of-plane direction is restricted so that a frictionless contact (fixed Y direction) and in-plane displacements (X and Z directions) were allowed, refer to Figure 3.2. Since the simulations were conducted by modelling the two weld passes on each side of the stiffener, the symmetry condition certainly could not be applied along the center line of the plate which is also the center line of the stiffener. However, if the two weld passes were conducted simultaneously, then the symmetry condition could have been a more applicable assumption, even though welding itself is not a symmetric phenomenon. Therefore the actual procedure followed for the welding in the benchmark was as mentioned above and did not qualify for symmetric conditions.

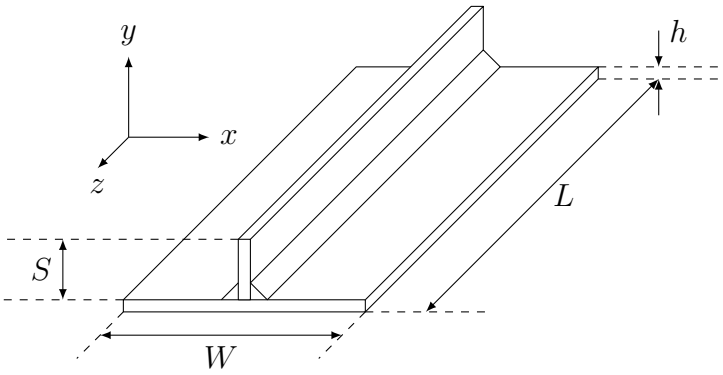

Figure 3.2: The ISSC2021v.3 benchmark [1] geometry of the stiffened plate. $L = 1000\,\text{mm}$, $W = 400\,\text{mm}$ and $S = 100\,\text{mm}$. The thickness of both the stiffener and base plate is $h = 5\,\text{mm}$. The weld has a leg of 7 mm. Note that in this project $L = 200\,\text{mm}$ was used.

3.2 FE-simulation

The simulation was carried out in multiple configurations which took into account varying types of heat source and clamping conditions for welding either side of the stiffener. A forward coupled thermo-mechanical simulation is done for all configurations.

Firstly, a heat source is modelled similarly to the actual welding scenario where the weld rod moves along the length of the stiffener. This is done by means of step-wise heat addition of 1000 °C moving heat source along the length of the weld from one end to the other by heating a few elements at a time in segments. This heating is done as three segments per weld, six segments in total for both right and left weld, and it is referred to as sequential heating. Another temperature simulation models the heat source as a simultaneous heat addition to all the weld elements along the length of the weld. This second temperature simulation configuration considers fusing the full length of the weld all at once and is referred to as simultaneous heating, and it is done for each side of the stiffener separately. These are the two heat source variations being considered and each weld pass is followed by a cooling period of 200 seconds before unclamping i.e., one side of the stiffener is welded first followed by a cooling period of 200 seconds and the other side is welded and cooled for 200 seconds before the plate is unclamped which marks the end of the simulation (the unclamping step is associated with only the mechanical simulation). It is important to mention that this cooling time only applies for all simulations except the ones done for the convergence analysis, which used a shorter cooling time.

The sliding clamp case leads to rigid body modes in the free XZ plane. To prevent this, two different methods were used. One of the methods was using *INERTIA RELIEF in ABAQUS [4] in the unconstrained degrees of freedom. Alternatively, a couple of nodes away from the clamps are constrained in the X and Z directions. Particular care needs to be taken in choosing these nodes to avoid undesirable model

behaviour during the simulation.

The resulting six configurations are summarized in the Table 3.1 below.

Since the model is subject to high temperatures and deformations, both material nonlinearity and geometric nonlinearity are considered during the simulations.

Table 3.1: Table of simulation configurations

Heat Source	Clamp Boundary Condition	Config No.
Simultaneous	Fully fixed	1
	Sliding with constrained nodes	2
	Sliding with inertia relief	3
Sequential	Fully fixed	4
	Sliding with constrained nodes	5
	Sliding with inertia relief	6

3.2.1 Simulation approach

The six configurations are simulated using ABAQUS [3] using the Hebbe cluster [5] at Chalmers Centre for Computational Science and Engineering (C3SE). The mesh convergence and many test simulations were done on the Chalmers computers via remote login. A text editor was used to define loads and BCs in an $*.inp$ file. The simulation approach for the project is as follows:
• The finite element (FE) mesh along with the CAD geometry are generated in the ABAQUS tool.
• Along with the FE-mesh, node and element sets are created for use in material, thermal, mechanical loading and boundary condition definitions. This data is saved as one $*.inp$ file which was used concurrently for all configuration simulations.
• Another $*.inp$ file with all the material data was created and consequently used for all simulations.
• A mesh convergence study is done for the thermal analysis in order to arrive at optimal mesh size based on temperatures of one particular location of the model.
• The thermal and mechanical loads are made in individual $*.inp$ file and used for all configuration simulations as required.
• A combination of the material and thermal/mechanical loading files is done in an other *mesh.inp* file by using ABAQUS commands to call and implement them during the simulation. This helps in discretizing the problem at hand and helps during error identification.
• Subsequently different $*.inp$ are made for individual configurations by using the thermal analysis results and use them for mechanical load simulation using the same above stated strategy.
• Comparison of results with the ISSC2021v.3 benchmark results are made with the results obtained through the project.

3.2.2 Boundary conditions

A forward thermo-mechanical simulation of the kind being performed requires two unique types of boundary conditions (BCs) that need to be defined for the FE simulation i.e., thermal and mechanical BCs.

3.2.2.1 Thermal BCs

The weld area is described as the area where the stiffener meets the plate, and the weld area consists of one side per pass. Figure 3.3 shows the weld area divided into segments. For each of the two weld passes, the welding heat source covers either simultaneously the whole weld pass area (simultaneous heating of all segments) or alternatively stepwise heating i.e., heat addition to one section of the weld after the other (sequential heating).

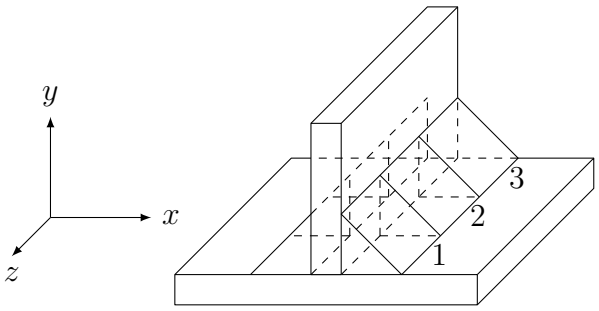

Figure 3.3: Sketch of the weld segments and numbering. The right side is number from 1 to 3 in negative Z, which also is true for the left side.

In the case of sequential heating, the weld sequence is reversed when the weld is to be performed on the second side of the stiffener i.e., 1,2,3 on one side and 3,2,1 on the other in Figure 3.3. This was implemented in ABAQUS by the use of field variables which deactivated not yet active segments by lowering the conductivity to zero. The effect of this can be seen in Figure 3.4 for both the simultaneous and sequential methods directly at the end of each welding pass. Every segment, regardless of welding method, was heated to 1000 °C for one second, meaning the total time for simultaneous welding was one second and for sequential welding three seconds per side.

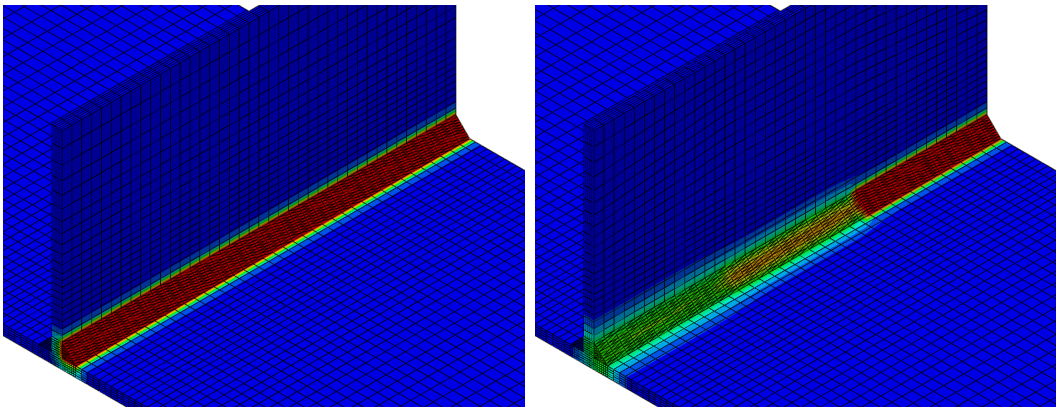

(a) Simultaneous welding. **(b)** Sequential welding.

Figure 3.4: The two different methods used for simulating the welding at the end of each welding pass. (a) is simultaneous for one second and (b) sequential for one second in each section for a total of three seconds. The red colour shows the maximum temperature of 1000 °C.

The natural convection to air was taken as $10\,\mathrm{W/(m^2\,°C)}$. The conduction to the table through a possible air gap is modelled with an increased convection coefficient of $300\,\mathrm{W/(m^2\,°C)}$ [6]. The convection was modeled using *SFILM [4] in ABAQUS.

The thermal boundary conditions are specified for all surfaces of the panel's plate, clamps and presented in the Table 3.2 below.

Table 3.2: Thermal BCs

Area domains	**Thermal BCs**
Weld area	Heat source (simultaneous or sequential) of weld area for only one side of the stiffener per pass (Dirichlet)
Free area in contact with air	Natural convection air room temperature (Neumann)
Bottom area in contact with table	Heat conduction table-plate (Neumann)

3.2.2.2 Mechanical BCs

The mechanical boundary conditions include those defined by the 4 clamps set at each side of the plate as shown in Figure 3.7

An initial assumption was made such that there is no contact between the plate and the table, and that the clamps alone are holding the plate in place. This is to avoid a complicated contact problem. Since it was noticed that the center line of the plate deflected downwards during the welding, a new boundary condition was defined on the bottom of the plate that restricted the deflection of the plate as a real table would. This is done via two rows of nodes at the bottom of the plate under the stiffener which constrains the plate so it remains fixed to the table along those rows (refer to Figure 3.7). These two rows of nodes which clamp the plate to the table represent the plate contact with the table at the center of the plate where the stiffener is located. During the unclamping step at the end after both right and

left weld passes are completed, it is needed to assign enough BCs on the model to avoid rigid body motions. This is done either by adding two constrained nodes or by using an ABAQUS subroutine called *INERTIA RELIEF [4].

3.2.3 Material properties and constitutive model

The material specified for the benchmark and used in this project is DH36 steel [1] which has a density of 7800 kg/m^3 [7]. Most of the temperature-dependant thermal and mechanical properties were taken from a fatigue analysis [6] which was conducted for a similar steel, S355. The specific heat and thermal conductivity were for the actual DH36 steel [8]. It was assumed that the properties for S355 are similar enough to the ones for DH36 to be used [9].

Figure 3.5 shows the temperature-dependent material properties that were used. Figure 3.5a shows the elastic modulus and Poisson's ratios. Specific heat and thermal conductivity are given in the Figure 3.5b, and the expansion coefficient in Figure 3.5c. Note that the drop in thermal expansion between 500 °C and 700 °C is associated with a material phase and volume change for which temperatures are not known exactly for DH36. All of these properties are the same for both the material in the plate and stiffener, and in the weld. The yield stress and hardening modulus are higher at room temperature for the weld, 470 MPa and 2.8 GPa respectively, when compared to the plate and stiffener, 390 MPa and 2.3 GPa respectively. For higher temperatures they are the same as shown in Figure 3.5d and 3.5e. The used hardening model was isotropic hardening [9].

During an actual welding procedure not all of the weld material is deposited at the same time. This was taken into account by first creating inactive elements for the whole weld region. During the simulations the conductivity was set to 0 W/(m °C) and the elastic modulus was set as 100 MPa for elements not yet deposited according to the welding procedure. This was done in ABAQUS by the use of *FIELD, VARIABLE [4] and defining different material properties for different values of the field variable. The use of *FIELD, VARIABLE allows activation of the deposited material as can be seen, for example, in Figure 3.6. When the weld elements are activated they are assigned a temperature of 1000 °C. This temperature was also set as the reference temperature for the coefficient of thermal expansion for the weld metal.

In Figure 3.6a the left weld was deactivated (dark blue) during the first heating pass and first cooling, while the right weld was active (orange). Figure 3.6b shows that the previously inactive left weld is now active and the temperature is distributed at the end of the second cooling step. In the Figure 3.4 as well, the sequential simulation keeps only the third segment of the right weld active while all other weld segments on the other side (refer to Figure 3.3) remain inactive.

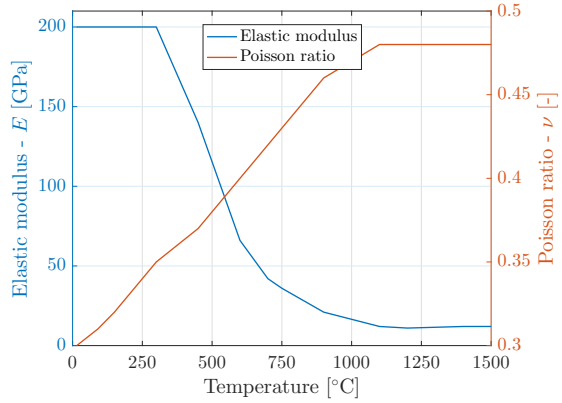

(a) Elastic modulus and Poisson's ratio for S355 [6].

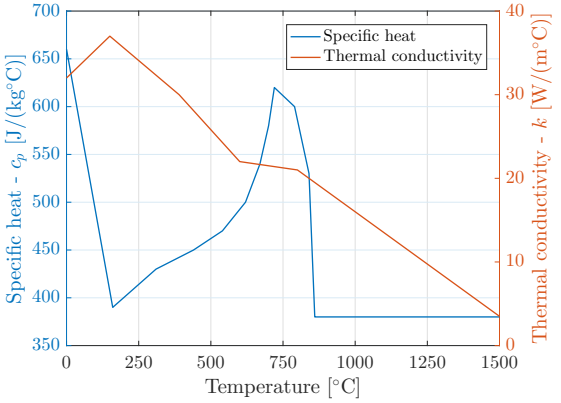

(b) Specific heat and thermal conductivity for DH36 [8].

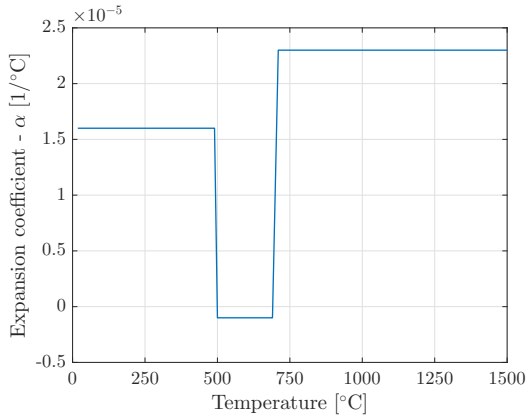

(c) Coefficient of thermal expansion for S355 [6].

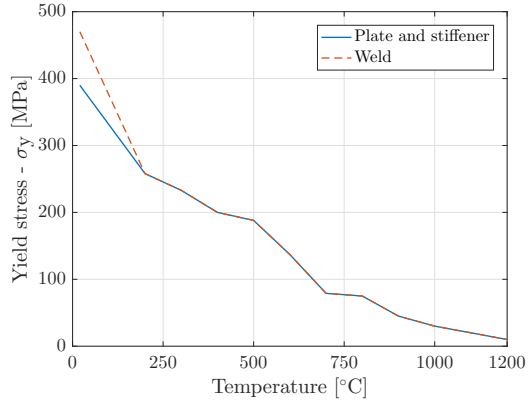

(d) Yield stress for the material S355 in the plate and stiffener and for the weld [6].

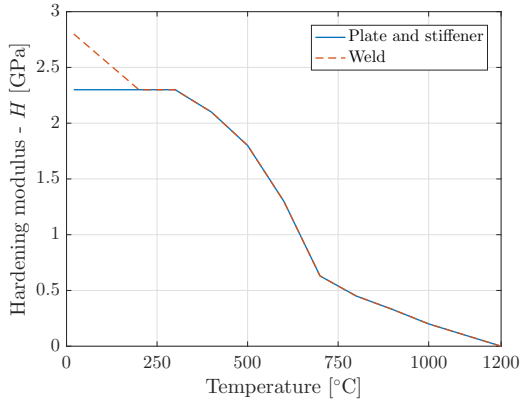

(e) The hardening modulus for the plate and stiffener from S355 and for the weld [6].

Figure 3.5: Temperature-dependent material properties for the stiffener, plate and weld [6, 8]

.

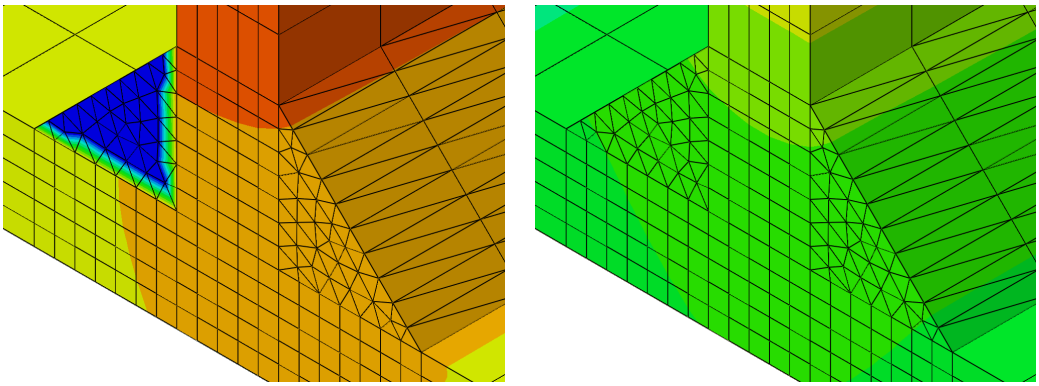

(a) Effect of field variable showing end of 1st cooling step

(b) Effect of field variable showing end of 2nd cooling step

Figure 3.6: Illustration and effect of field variables during simulation

3.2.4 Mesh geometry and elements

The same mesh was used for both the thermal and mechanical simulations. This mesh consists of linear hexahedral and linear tetrahedral solid elements. The hexahedral elements are used to model the plate and stiffener except the welding joint. The weld is triangular in cross section and is modelled only with linear tetrahedral elements. For the thermal simulations the 8-node hexahedral and 4-node tetrahedral linear elements used are DC3D8 and DC3D4, whereas for the mechanical simulations element types used are C3D8 and C3D4 are used respectively as per ABAQUS formulation.

The mesh size is determined from a convergence analysis where the temperature variation in time is simulated for a point seen in Figure 3.7 located 30 mm away from the weld in X direction, and at the center line (CL), which is at location $Z = 100\,\text{mm}$ for the 200 mm simulated plate and stiffener. To reach a converging solution faster, it is important to have a more overall refined mesh, but particularly more refined in the weld area. As a rule of thumb there are at least four elements needed through the weld for good weld mesh, meaning along the distance between the right angle corner and the hypotenuse, as shown in Figure 3.7 more were used. In Figure 3.7 the red nodes at the bottom and top corners of the plate (8 nodes) are used to model the clamping condition, either sliding or fully fixed as described in section 3.2.2.2. The red nodes under the stiffener indicates nodes that were constrained in Y direction depicting the table.

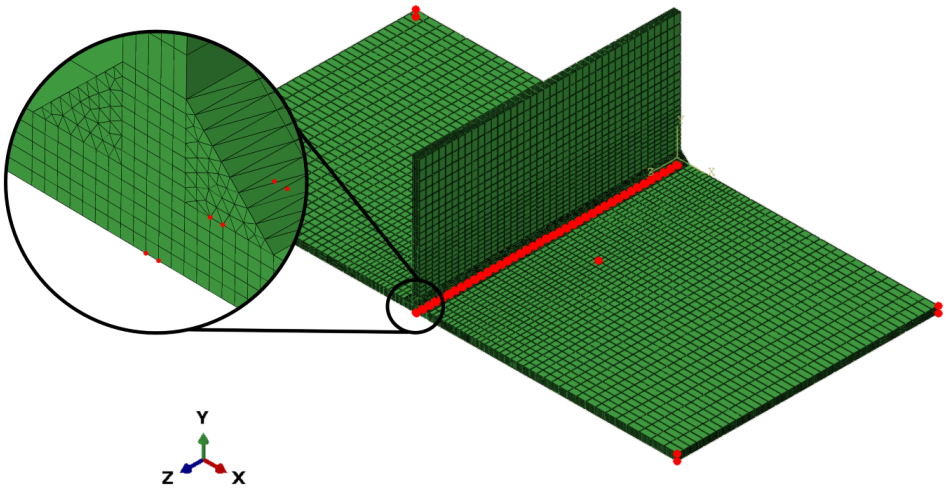

Figure 3.7: Mesh for the stiffened panel with the corner nodes on the plate clamped. The red nodes under the stiffener are constrained in Y direction only. Mesh convergence was performed on the single node adjacent to the weld. Note that the plate and stiffener are 200 mm long (Z direction).

4 Results

4.1 Convergence

Different base mesh sizes and gradients are used to establish a reasonably converged mesh using thermal simulations. The base mesh size of the elements represents the size of elements located in the near-field, up to 30 mm away in the normal direction of the weld edge (X direction) and mesh grading was applied in the same direction from the near field to the edge of the plate. The maximum element size for the grading used is the base mesh size plus either 3 mm or 8 mm. The convergence analysis was particularly done only with a simultaneous heat source (not sequential), welding on only one side and with a shorter cooling time of 50 seconds. The temperature distributions are compared on the same side of the plate as that of the welding. In Figure 4.1 the convergence of the thermal simulations are plotted for a node located at 30 mm away from the weld in X direction, at the center line (CL) in Z direction (Z=100 mm), see Figure 3.7. As can be seen in the Figure 4.1 several lines for more refined meshes follow about the same path and can therefore be assumed to be reasonably converged. Based on that assumption of reached convergence for some of the refined meshes, the chosen mesh has an initial base size of 3 mm for the elements located in the near-field up until the beginning of the far-field, and additionally a base size of 10 mm for the elements located at the end of the far-field (far end of the plate in X direction). The base mesh size and the maximum element size of the far field is chosen such that the aspect ratio does not cross a value of 10 and to avoid issues within the mechanical simulations by having too long elements in the model. The final node count for the chosen mesh is 31200.

Another aspect of the convergence analysis is the computational time based on the number of nodes and base mesh size (or alternatively number degrees of freedom). In Table 4.1, the run time refers to the duration of the thermal simulations for different meshes and which were carried out on a local computer i.e., on computers at Chalmers in the M - computer rooms rather than on the cluster.

Table 4.1: Run times on local computers against the No. of nodes in model: Mesh Convergence thermal analysis.

Base mesh size+3 mm gradient			Base mesh size+8 mm gradient		
Base mesh size	No. of nodes	Run time	Base mesh size	No. of nodes	Run time
2 mm	119000	41 min	2 mm	100000	30 min
3 mm	62000	20 min	3 mm	54000	15 min
4 mm	40000	15 min	4 mm	36000	10 min
5 mm	27000	10 min	5 mm	25000	7 min

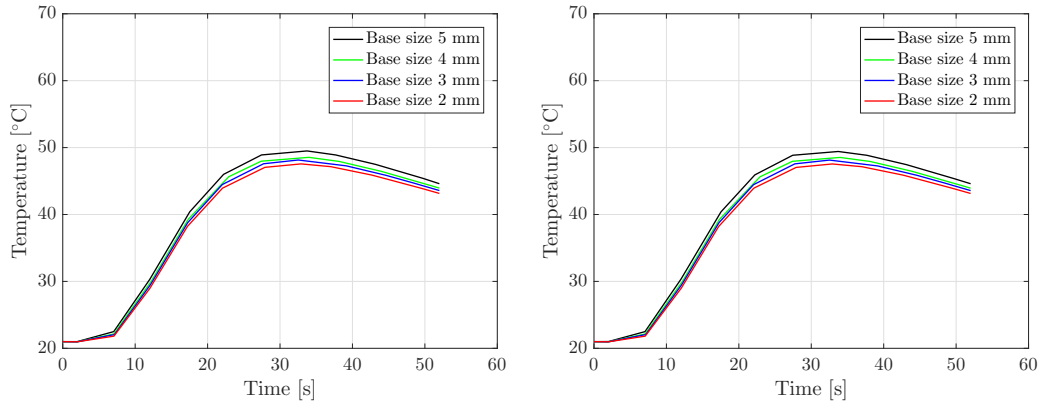

(a) Convergence using meshes with base mesh size + 3 mm.

(b) Convergence using meshes with base mesh size + 8 mm.

Figure 4.1: Convergence of thermal simulations for different base sizes and gradients 30 mm from the weld. Figure (a) used a mesh with different base sizes and a gradient from the base size to the base size plus 3 mm. The same is true for (b) but with 8 mm instead.

4.2 Thermal simulations

Based on the established converged mesh (base size of 3 mm and the gradient from 3 mm to 10 mm in the far field) the thermal simulations are carried out. Figure 4.2 shows the final temperature field for both the simultaneous and sequential heat source at the end of simulation i.e., at the end of cooling step post second weld. Figure 4.2 shows that the distributions are very similar but the maximum temperature is slightly higher for the simultaneous heat source, 52.6 °C, compared to the

sequential heat source, 52.4 °C. This small difference in the final maximum temperature is due to the fact that the sequential heating generates a higher temperature loss through heat transfer i.e., via conduction and convection after each one of the three segmented heating per weld pass before the start of the cooling step. However, the simultaneous heat source does the welding in one step before the start of the cooling step. For the sequential case, the actual cooling step begins only after the three segments of the weld have been each heated, as opposed to the simultaneous case where the cooling step occurs right after simultaneous heating of one full weld.

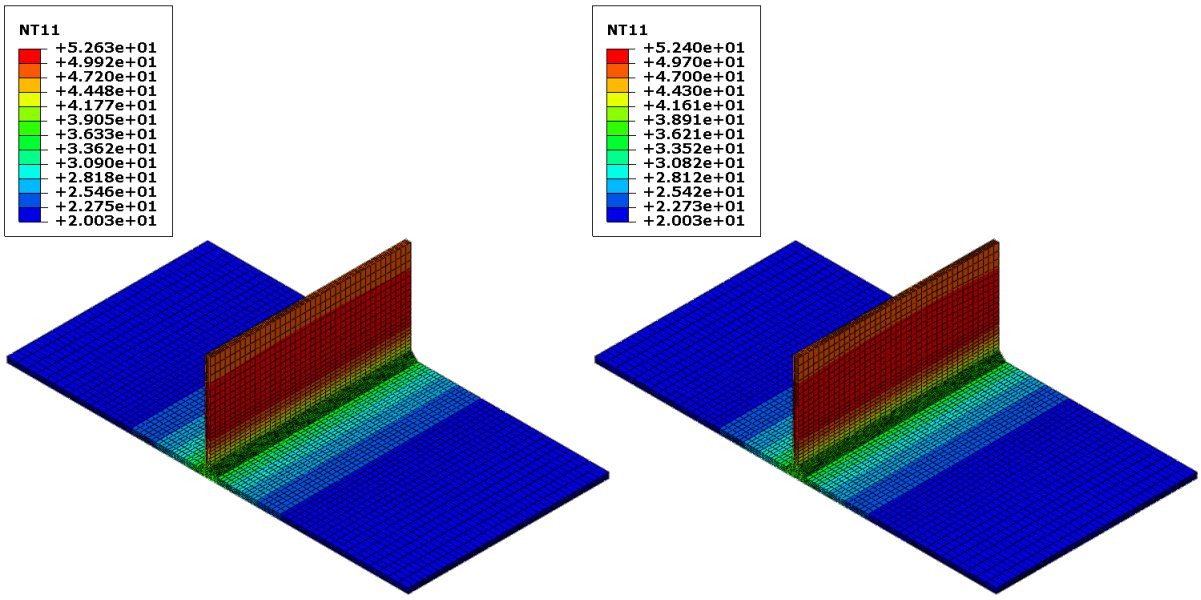

(a) Simultaneous heat source. **(b)** Sequential heat source

Figure 4.2: The final temperature distribution in Celsius for simultaneous and sequential heating.

4.2.1 Cooling time between 800 °C and 500 °C compared to analytical solution

Another interesting comparison between results would be the cooling time from 800 °C to 500 °C between the simulations and an analytical formulation. The analytical solution of the heat conduction equation for a 2D thin plate, with a moving heat source and constant, temperature independent material properties can be found in Equations 1.22 and 1.23 in [10]. To make such a comparison, a node is chosen along the center line and in the center of the right weld which is the first side welded, and then for that node the temperature variation over time is plotted for both simultaneous and sequential heating. The results are plotted in Figure 4.3. In Figure 4.3 it is interesting to notice the time required for the temperature to drop from 800 °C to 500 °C and to compare it to an analytical solution. In Figure 4.3 it is also noticeable in the beginning that the temperature starts at 1000 °C (heat source temperature), but with one second delay for the sequential because the node is in the second segment and it starts to heat up after one second. After the initial heating,

the right weld starts to cool rapidly in the beginning and slowing down at lower temperatures. Another observation is that at about 200 s (exactly at 201 s and 203 s for simultaneous and sequential case) the next side is welded and a second increase in temperature occurs. During the second weld pass, the temperature peak is much lower because the heat source is then applied on the other side of the stiffener, and heat is then conducted not only to the plate and stiffener but also to the previously deposited weld.

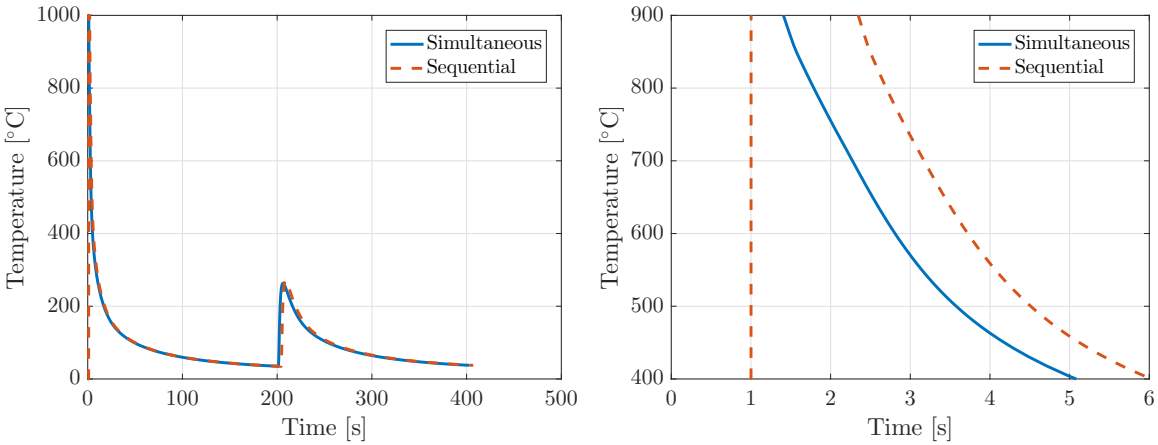

(a) Temperature during the whole procedure.

(b) Cooling between 800 °C and 500 °C.

Figure 4.3: Temperature over time for one node in the center of the first weld along the center line.

In Table 4.2 the cooling time between 800 °C and 500 °C for the same node as in Figure 4.3 is compared to an analytical result [10] based on the benchmark [1]. They are similar in time, but the simulated values are smaller. There is also a small difference between the simultaneous an sequential welding, with the sequential having a slightly longer cooling time.

Table 4.2: The time for cooling between 800 °C to 500 °C for the simultaneous and sequential heating methods compared to analytical result [10].

Analytical [s]	Simultaneous [s]	Sequential [s]
4.80	1.75	1.78

4.3 Mechanical simulations

The mechanical simulations were carried out for the same mesh and with the thermal analysis as input. The mechanical simulations are carried out for all the six different configurations referred to previously in Table 3.1.

4.3.1 Fully clamped

Figure 4.4 shows the residual total deformation field for the fully clamped condition. It is observed that the deformation for the simultaneous heat source is higher than the sequential heat source. It is also observed from the Figure 4.4 that the deformation pattern varies differently for the simultaneous and sequential heat sources. Earlier in the temperature field comparison (see Figure 4.2), it can be noted that the temperature was lower for the sequential heat source compared to the simultaneous heating due to a longer convective time. This loss of temperature during the sequential heating also accounts for some stress relief during the mechanical simulation after each one of the six segmented weld passes. Therefore the residual thermal stress is lower for the sequential heat source simulation, so is the magnitude of the displacements, at the end of the simulation i.e., after unclamping, see Figure 4.4. Skewed deformation of the stiffener and plate is clearly asymmetric in the sequential heating case as opposed to the seemingly more symmetric deformation in the simultaneous case. There is a small difference in max displacement, meaning that the simultaneous has 1.374 mm and sequential 1.290 mm. The difference of displacement magnitude between the heating types is most observable in the stiffener as the sequential heating has more time for convection to air than in the case of the simultaneous heating.

It is to be noted that this simulation was done with a plate and stiffener 200 mm long. The deformation seems to be small but the deformation will probably be larger if the simulation is carried out for a plate of 1000 mm long and more segments are used for the sequential welding heat source.

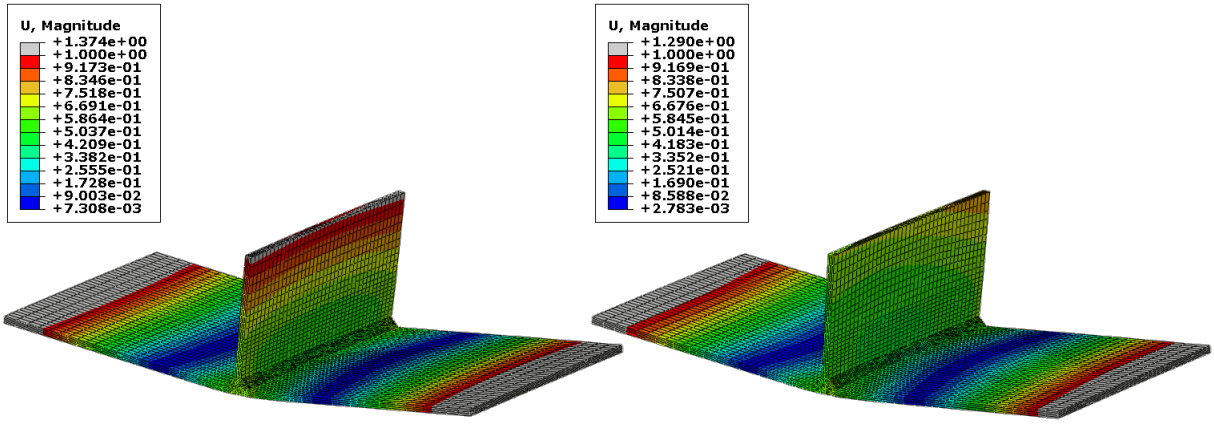

(a) Simultaneous. **(b)** Sequential.

Figure 4.4: Final residual total deformation field showing displacements in mm for simultaneous and sequential heating with the fully clamped BC.

4.3.2 Sliding at clamps using constrained nodes

In this configuration to prevent the rigid body motions in the unconstrained X and Z degrees of freedom, two additional nodes as shown in Figure 4.6 are fixed also only

in X and Z degrees of freedom. These two nodes are chosen such that they do not affect the general behaviour of the simulation. From the Figure 4.5 it is seen that the deformation is higher for the simultaneous heat source than for the sequential heat source as has been the case with the previous configuration. It is also seen from the Figure 4.5 that the pattern between the current configuration differs from the fully clamped one in a way that the deformation is higher for this configuration over all due to the fact that throughout the simulation the X and Z degrees of freedom are free at the clamps but constrained on one edge of the plate. This also accounts for the highly asymmetric deformation of the stiffener from the fully clamped condition. Finally, there is a difference in max displacement, the simultaneous case has 1.783 mm and sequential 1.548 mm.

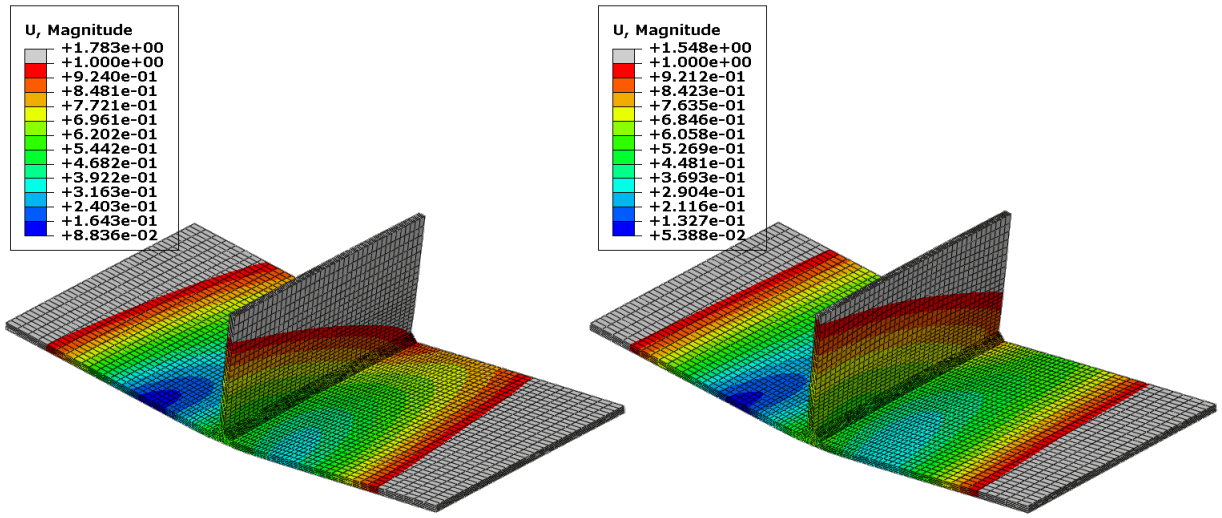

(a) Simultaneous. **(b)** Sequential.

Figure 4.5: The final displacement distribution in mm for simultaneous and sequential heating with the sliding BC (degrees of freedom free in X Z directions) with two additional constrained nodes implemented. There is difference in max displacement

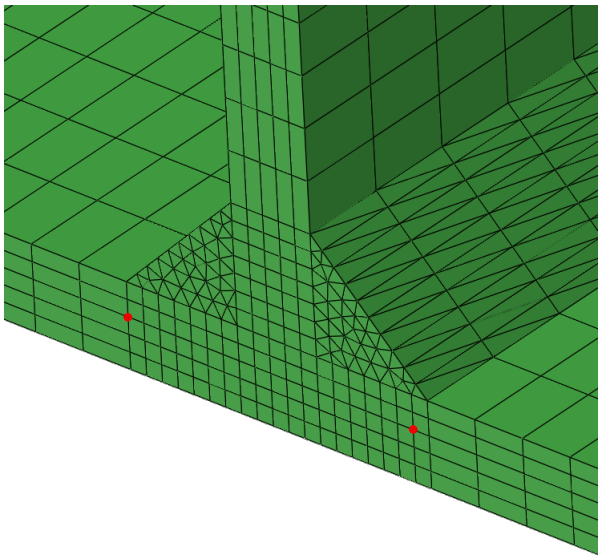

Figure 4.6: The two nodes constrained.

4.3.3 Sliding at clamps using inertia relief

The other method used for preventing the rigid body motions in the sliding clamps configuration were the X and Z degrees of freedom which are free (not fixed by clamping) is to use inertia relief. This method uses the ABAQUS subroutine called *INERTIA RELIEF [4] during each heating and cooling step for the unconstrained degrees of freedom of the clamps. The resulting displacements can be seen in Figure 4.7. The displacements for the simultaneous case are slightly higher than for the sequential case in line with the other configurations. It can also be noted that, compared to Figure 4.5 the deformations in this configuration are much more symmetric. Moreover, a difference in max displacement is observed, the simultaneous case has 1.748 mm and sequential 1.688 mm.

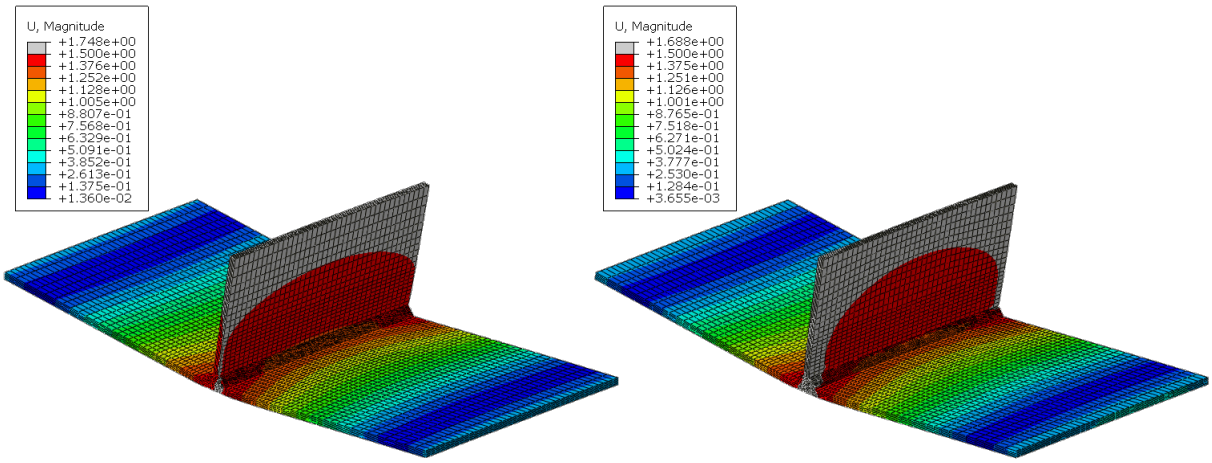

(a) Simultaneous. **(b)** Sequential.

Figure 4.7: Final residual total deformation field in mm for simultaneous and sequential heating with the sliding BC (degrees of freedom free in X Z directions) with inertia relief implemented throughout all heating and cooling steps

4.3.4 Plate deflection compared to analytical solution

Figure 4.8 shows a comparison of the final displacements in Y direction for the plate at the end after unclamping for the six different configurations as in Table 3.1 which resembles a V-shape. The displacements are taken for points equally spaced on either side of the stiffener starting from the weld, on the top face of the plate and at the center line of the plate along the weld direction (100 mm in Z direction). The simulations are also compared to an approximate solution for the angular distortion resulting from welding of a steel stiffener and plate based on Figure 19 in [11], where w is the weight per length of the weld in g/cm and t the plate thickness. Note that all of the simulations and the analytical solution have similar displacements. The displacements on the right side are slightly higher than the ones on the left, creating a slightly asymmetric V-shape. The right side was the first to be welded and the left the second. For the fully fixed clamping case, the simultaneous (sim) heat source generated higher displacements than the sequential (seq) heating. For both of the sliding clamping conditions (Inertia relief and constrained nodes), only constrained in Y direction, the displacements were higher for the sequential heating (seq) instead and lower for the simultaneous (sim).

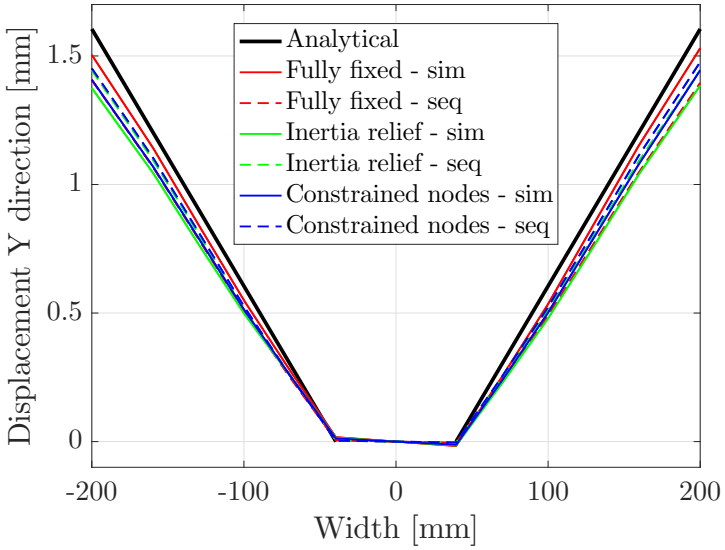

Figure 4.8: Comparison at the end after unclamping of the produced V-shape from simulations with analytical formulation [11]. Note that the displacements are similar on both sides with slightly higher values on the right, resulting in a slightly asymmetric V-shape.

5 Discussion

5.1 FE-model and sources of limitations

The geometry of the weld fillet is in reality irregular and only approximately triangular in cross section. Nevertheless, it is modelled as a triangular shape in a cross section of the plate and stiffener (see Figure 3.7 in Mesh geometry and elements section). Depending on the nonuniformity of the real cross section, this approximation may be adequate. Further study is required. A second concern is that of the elements order, which are chosen to be linear (hexahedral and tetrahedral), along with the mesh size in terms of how many elements are used for the simulation. Third, the clamping boundary conditions are also an approximation of actual clamping conditions. The clamping footprint (contact area) is taken to be as a single node on top and bottom surfaces. In reality the clamps would cover a small area each one of them. The clamping location was set at approximate locations estimated by looking at the benchmark in Figure 3.1 in the Geometry section.

5.2 Convergence

A convergence study was performed and the results in Figure 4.1 show for different base mesh sizes the thermal convergence at one node located in the near-field, see

Figure 3.7. That convergence analysis shows the effect of different mesh sizes for the near field and a mesh with increasing size thereafter. All the combinations of base mesh size and the mesh grading as in 4.1 had comparable temperatures at the near field location as in Figure 4.1. Though the mesh could have been made coarser, in the interest of compatibility for mechanical simulations, a final mesh was chosen from the combinations which had a maximum element aspect ratio of around 10. The assumption is that this mesh is sufficient for the mechanical simulations. Also, the mechanical simulations require finer mesh as the load steps required would be small for such a simulation to accurately take into account all the thermal data, as loads. And this in turn translates into high simulation times. Time did not permit a detailed mesh convergence for the mechanical analysis which would take into account the load steps, base mesh size in the near field and mesh grading in the far field.

5.3 Thermal simulations

In Figure 4.2 the final temperature distribution after two weld passes and final cooling are shown for the simultaneous heating and the sequential heating. The distributions are at this stage very similar, but with a small difference in maximum temperature. The simultaneous heat source simulation had a maximum temperature of 52.6 °C and the sequential of 52.4 °C. This difference is probably due to that reason the sequential simulation had slightly more time to cool because each of the three segments were activated for one second each, while for the simultaneous heat, all of the segments on one side were activated at the same time for one second. This would mean that in case of sequential heating the previous segments have time for conduction and convection while the next segment is heated and therefore the sequential heating should be slightly cooler. One important difference also influencing the temperature distributions is the total energy input to the system. For the used methods it should be a similar amount because the simultaneous heat source heated the whole weld for one second and the sequential one heated a third of the weld for one second three times per weld. Thus the total amount of supplied energy should be very similar. Some small difference might still appear given how the temperature conducts out from the weld and into the plate, and given that the convection also has an effect. Both of these factors have for the sequential heat source case probably a small effect given the heating time.

The temperature distribution will probably be highly dependent on the number of segments used. In this project only three per side is used due to limitations in time and resources. More segments would mean more realistic simulation of a moving heat source because each segment would be shorter an closer to the size of the welding head. This effect will also probably be even more noticeable for the full length geometry of 1000 mm specified in the ISSC2021v.3 benchmark [1]. Another important factor determining the temperature distributions is the temperature used either for the heated segment(s). In this project 1000 °C is used. In reality, the added weld material is in a melted state and has a temperature of approximately 1500 °C. This will probably give higher temperatures and especially for the longer

plate a more pronounced difference between simultaneous and sequential heating methods.

The conduction to the table through the underside of the plate is modelled as convection a *SFILM ABAQUS function [4] which acts as a film stuck to the surface which is always at certain temperature. This is a limitation because the plate might bend during the welding and cause some parts of the plate to not be in contact with the table and then loose the higher value of convection. This requires including a complex contact condition a fully coupled thermal mechanical analyses to take this effect into account. Different contact distributions from the mechanical analysis affects the BCs to be added in the thermal analysis. So they have to be run in parallel fully coupled. This is beyond the scope of the simplified approach to this project. Another effect of the thermo-mechanical coupling is that heat generated from the deformation is not included in the thermal simulations. This effect is probably very small for the deformations calculated.

The whole welding procedure can be seen in Figure 4.3a for one node in the center of the right weld, the side that is welded first. The temperature is initially 1000 °C but with one second delay for the sequential heating. This is due to the location of the node is in the second weld and it starts to heat up after one second. After reaching the maximum the temperature quickly decreases and the decrease slows down for lower temperatures. After 200 s of cooling, the second side is welded and this is reflected in the graph by a rapid increase in temperature but to a lower maximum. This is because the node is not directly heated and only some of the applied heat on the other side will conduct to it. Therefore the temperature will be lower. During the whole procedure the temperatures for the simultaneous and sequential heating cases are similar, but with a small difference in time, especially noticeable in Figure 4.3b. This is because the simultaneous welding is one second per side and the total time for one side during the sequential is three seconds. This means that some differences will occur.

5.4 Cooling time between 800 °C and 500 °C compared to analytical solution

An analytical comparison can be found in Table 4.2 between the cooling time from 800 °C to 500 °C and that between the simultaneous and sequential heating. These are also compared to an analytical result [10]. The cooling effect can also be seen in Figure 4.3b. The simulated cooling times for the sequential and simultaneous case are lower than the analytical but still in the same range. This difference is probably because the analytical result is based on the benchmark [1] and especially caused by the welding speed used. The time to weld one side in the benchmark was much longer than for all the six simulations configurations. If a higher welding speed were to be used for the analytical result, a lower cooling time would be obtained. This shows that the simulations produced reasonable results which were consistent with the real world. One reason why the sequential cooling time is slightly longer

is because the welding procedure is longer than for the simultaneous case. The simultaneous heat source is applied at the same time for the whole weld while the sequential in different steps. This means that while the middle segment is cooling some heat can be conducted from the following segment that is welded and therefore the cooling can be slightly drawn out.

5.5 Mechanical simulations

As discussed earlier, a contact condition between the bottom of the plate and the top of the table is not defined to avoid introducing a complex contact problem in the mechanical analysis. Based on initial simulations the plate was seen to deflect downwards at the center line (CL) under the weld metal. In order to prevent this downwards deflection of the plate, two rows nodes are fixed in Y direction are introduced in place of the contact, see Figure 3.7. This probably induces some unrealistic behavior as the effect of such BC is different from a contact problem, which is much closer to reality. Yet even if the actual displacements were small for such a contact problem, this method of constrained nodes could be sufficient.

The final displacement fields after unclamping for the different heating methods and clamping conditions can be seen in Figures 4.4, 4.5 and 4.7. The maximum displacements are similar in magnitude for all cases. This is true especially for the cross section along the center line which can be seen in Figure 4.8. What this suggest is that for this length of plate the methods used does not effect the magnitude of maximum displacements. One large difference however is the shape and distribution of these displacements. The cases fully clamped and sliding contact with inertia relief are nearly symmetric along the center line for both simultaneous heating and sequential heating. The case with sliding contact and two constrained nodes have a clear asymmetric behaviour along the same line. This is probably due to the constrained nodes only being placed on one side of the plate. For both of the other two cases the problem is more symmetric because the clamps are added to the corners and therefore symmetric. The inertia relief used a location along the center line under the stiffener. This will probably also create more symmetric behaviour. For a longer plate such as the one specified in the ISSC2021v.3 benchmark there would probably be a much more noticeable asymmetric behaviour for the sequential heating method, especially if more segments are used and a more realistic temperature applied. The displacements would then probably have a large difference between the simultaneous and the sequential cases. The sequential case should have different amount of displacement depending on the position along the Z axis. This can barely be noticed in Figure 4.4. The displacements for the simultaneous are almost the same along the Z axis. For the sequential they depend more on the Z axis and the left side of the plate have slightly higher displacements for positive Z. This is because a larger part is over 1 mm on the positive Z end than in the negative Z end. This effect would probably be much more distinguished for a longer plate.

5.6 Plate deflection compared to analytical solution and experimental result

In Figure 4.8 the simulated Y displacements for the cross section at the center line (CL) are compared to an approximate analytical angular distortion for fillet welding of a stiffener [11]. All of the displacements are similar in magnitude and behaviour. Comparing the simulated results with the experimental results in [1] show a similar behaviour, but not magnitude of deflection. Those experimental results shown in [1] were specifically carried out for pulsed gas metal arc welding (GMAW) of a 1000 mm welded stiffened panel with an unclamping and reclamping procedure in between the two weld passes. Furthermore, they are here presented in terms of the four corners deflections (Y direction displacements) in Table 5.1.

Table 5.1: Experimental values for the vertical deflection of the 1000 mm plate in the four corners relative to the bottom left corner [1].

	Left	Right
Top	15 mm	7 mm
Bottom	0 mm	13 mm

In Table 5.1 the deflection values for the experimental results are relative to the bottom left corner. The difference in magnitude of vertical deflection between the experimental and simulated values for sequential heating is clear. The deflection for the simulation is between 1 mm and 2 mm. In both cases a similar behaviour is observed because both show skewness, but more clearly in the experimental data. This is partly because of the longer plate, more complex welding steps and different clamping procedure for the experimental results. So the magnitude is different, but the behaviour is similar. The fact that the simulated displacements are similar to the analytical solution and experimental results shows that the simulations gave reasonable results. The displacements are also slightly higher on the right side, which is the one that is first welded. The difference is small, but because of the asymmetric welding procedure, the resulting displacements should also show some asymmetric behaviour. It might also be expected that the first side welded ends up with higher displacements. Actually, for almost all of the six simulations configurations the first side welded (right) ends up with higher displacements, probably because the other side's weld does not exist yet. When the first side (right) is welded, the left side is not active and cannot prevent much of the displacements because of a reduced stiffness. That being said, during the welding of the other side (left), the first weld can then contribute to resisting the displacements and therefore slightly lower values for the distortion (displacements) are obtained.

Another important observation is that there is no clear correlation between the type of heat source (simultaneous or sequential) and the resulting displacements. For the fully fixed clamping condition in Figure 4.8, the simultaneous heat source gave higher displacements than the sequential. For both of the cases with sliding clamping using inertia relief and constrained nodes, the opposite was true. In those

cases the sequential heating resulted in higher displacements. This might be a general behaviour for the sliding clamping condition, or an effect of the chosen cross section or of the choice of the nodes which are used for constraining and preventing rigid body motion (see Figure 4.6).

6 Conclusion

The project was intended to assess several simplified approaches based on forward coupled thermal mechanical simulations. The length of the plate and stiffener simulated is 200 mm instead of their actual 1000 mm length as in the ISSC2021v.3 benchmark [1]. On a side note, the heat source temperature was considered to be 1000 °C rather than as high as the actual temperature of the weld when deposited, i.e around 1500 °C. Thermal simulations with a higher heat source temperature would render higher temperature fields distributions and for the mechanical simulation higher displacements.

Some of the primary conclusions from this project are based on the behaviour of the model depending on the heating method and the clamping conditions along with methods used to prevent rigid body motion in some cases.

The final temperature distribution field is asymmetrical in the case of the sequential heating due to the additional time for conduction and convection available as the subsequent welds segments are heated. This has some significant changes in the mechanical simulation in the way of the final deformation field of the sequential heating model produces a skewed deformation at the ends of the plate. This skewed deformation follows the pattern of deformations presented in the benchmark [1]. However, the simultaneous heating has symmetrical final temperature fields and deformation fields at the end of the simulation, which is not a behaviour observable in the benchmark's results. It was also found that the sequential heat source gave slightly a more realistic shape of the final deformed state, than the simultaneous case.

Another observation was that the modelling of the clamping conditions also played a major role in the final deformation behaviour of the plate and the stiffener. This gives an insight on what the actual behaviour of the model will be when the clamps used in the benchmark have similar behaviour as that of this study. The fully fixed clamping condition shows the complete effect of the final thermal fields on the final deformation field and its dependence on the heat source type.

The sliding clamp conditions showed the effects of the methods (inertia relief or constrained nodes) used to prevent rigid body motions in the unconstrained degrees of freedom. This also played a pivotal role in the final deformation field. The inertia relief method showed the familiar symmetric deformation fields as that of the fully fixed condition and the constrained nodes configuration gives a completely asym-

metric final deformation field which might be not a completely realistic result.

The simulations were carried out on a shorter plate that was 200 mm long, and that was enough to show significantly distinctive behaviors of the results, although the magnitude of deformation for all the configurations were close to each other. Considering all the aforementioned differences between the configurations for the mechanical simulations,these differences will be magnified when the plate is scaled to a 1000 mm due to the same effects.

Finally, the time taken (Δt) for cooling from 800 °C to 500 °C at a certain node in the mesh at the center-line and near the weld was compared to an analytical solution. Another comparison between the simulation results and an analytical solution was done in terms of plate deflection in Y direction.

6.1 Future work

A future investigation of the welding process of this stiffener to the plate, could be simulated with a much more refined mesh. The simulation geometry could take into account the full 1000 mm length of the plate and stiffener according to the benchmark, and incorporating irregularities in the weld. Furthermore, an improved mesh grading of the plate, a finer mesh in the welds and a coarser meshing towards the ends of the stiffener and plate are needed and recommended.

Another important future contribution to the benchmark would be to segment each one of the two welds into more than three segments when simulating the heat source as being sequential. Although this is a valid option, an even more realistic consideration of the moving heat source in terms of simulation, would be to model it more accurately as actually a moving heat source generating a heat flux. Modelling the moving heat source within the weld as a heat flux rather than a constant heat source would be highly more accurate. That would take into account the gradual heating of the weld area, rather than with full segments like it is done currently with a sequential heat source. Finally, adding the contact condition between the table and plate would also generate more accurate results for the mechanical simulation.

Bibliography

[1] S van Duin. *Outline of the welding deformation benchmark, ISSC 2021V.3 Materials & Fabrication. Personal communicaton 2020.*

[2] L Josefson and M McDill. *Deformations in welded panels. Presentation to TME131 personal communication 2020.* Gothenburg.

[3] *DASSAULT SYSTÈMES - ABAQUS*. May 21, 2020. URL: `https://www.3ds.com/products-services/simulia/products/abaqus/`.

[4] *Abaqus Keywords Reference Guide*. May 21, 2020. URL: `http://130.149.89.49:2080/v2016/books/key/default.htm`.

[5] *Hebbe cluster, Chalmers Centre for Computational Science and Engineering (C3SE)*. May 21, 2020. URL: `https://www.c3se.chalmers.se/about/Hebbe/`.

[6] B L Josefson, J Alm, and J M J McDill. "Simplified FEA models in the analysis of the redistribution of beneficial compressive stresses in welds during cyclic loading". Proceedings of the 37th International Conference on Ocean, Offshore and Arctic Engineering. Madrid, Spain, June 17, 2018.

[7] J Su, W Guo, W Meng, and J Wang. "Plastic behavior and constitutive relations of DH-36 steel over a wide spectrum of strain rates and temperatures under tension". *Mechanics of Materials* 65, 2013, pp. 76–87.

[8] D Micallef, D Camilleri, A Toumpis, A Galloway, and L Arbaoui. "Local heat generation and material flow in friction stir welding of mild steel assemblies". *Proceedings of the Institution of Mechanical Engineers, Part L: Journal of Materials: Design and Applications* 230.2, 2016, pp. 586–602.

[9] L Josefson. *Personal communication 2020.*

[10] K E Easterling. *Introduction to the physical metallurgy of welding*. 2nd ed. Oxford; Boston: Butterworth Heinemann, 1992. 270 pp.

[11] G Verhaeghe. *Predictive formulae for weld distortion: a critical review*. Abington Publishing special report. OCLC: 632811768. Cambridge: Abington Publ, 1999. 90 pp.